SINTEF
PROCEEDINGS
2

Proceedings of the 12th International Conference on Computational Fluid Dynamics in the Oil & Gas, Metallurgical and Process Industries

Progress in Applied CFD – CFD2017

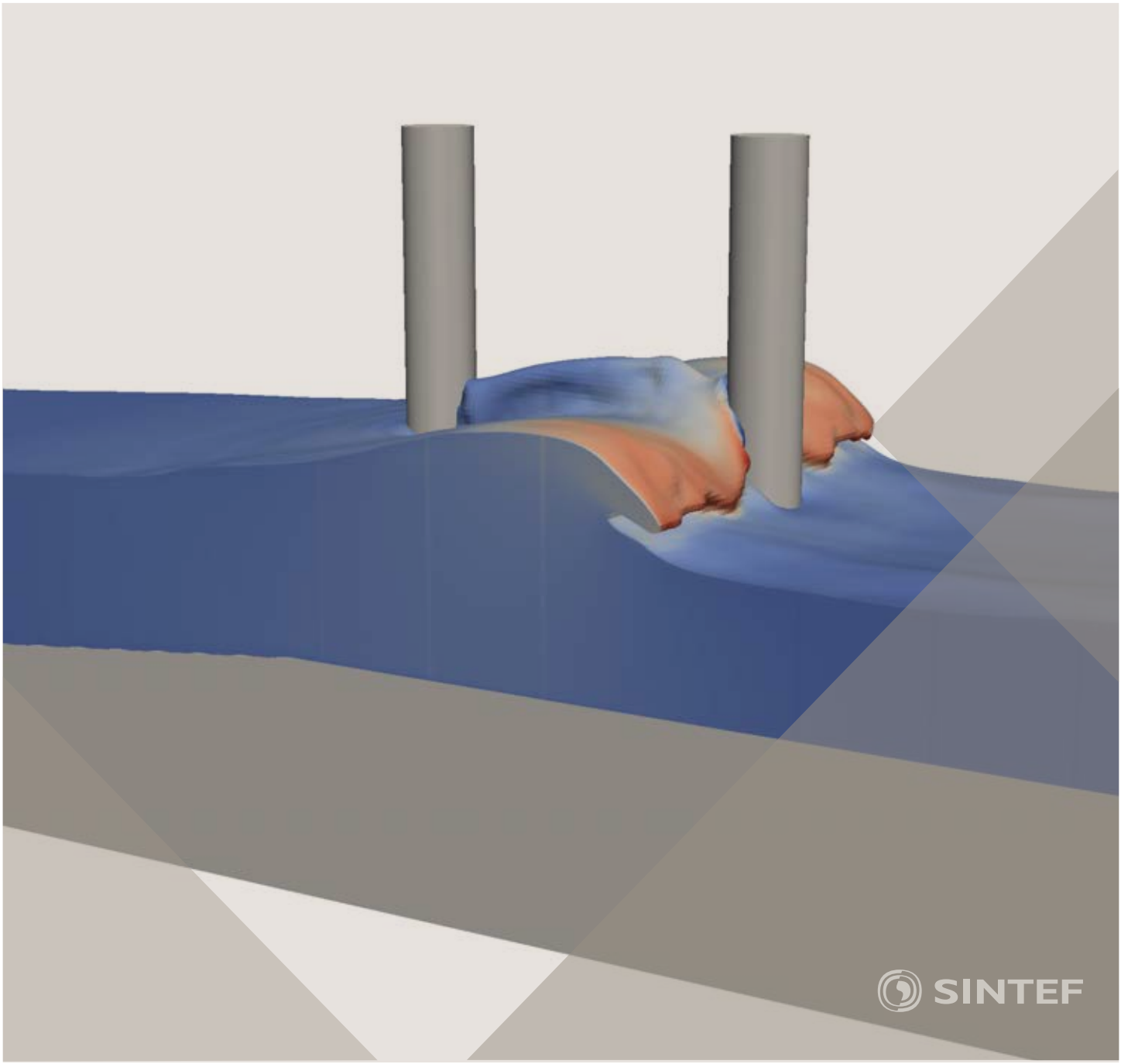

SINTEF Proceedings

Editors:
Jan Erik Olsen and Stein Tore Johansen

Progress in Applied CFD – CFD2017

Proceedings of the 12th International Conference on Computational Fluid Dynamics in the Oil & Gas, Metallurgical and Process Industries

SINTEF Academic Press

SINTEF Proceedings no 2
Editors: Jan Erik Olsen and Stein Tore Johansen
Progress in Applied CFD – CFD2017
Selected papers from 10th International Conference on Computational Fluid Dynamics in the Oil & Gas, Metallurgical and Process Industries

Key words:
CFD, Flow, Modelling

Cover, illustration: Arun Kamath

ISSN 2387-4295 (online)
ISBN 978-82-536-1544-8 (pdf)

SINTEF Academic Press
Address: Forskningsveien 3 B
PO Box 124 Blindern
N-0314 OSLO
Tel: +47 73 59 30 00
Fax: +47 22 96 55 08

www.sintef.no/byggforsk
www.sintefbok.no

SINTEF Proceedings
SINTEF Proceedings is a serial publication for peer-reviewed conference proceedings on a variety of scientific topics.
The processes of peer-reviewing of papers published in SINTEF Proceedings are administered by the conference organizers and proceedings editors. Detailed procedures will vary according to custom and practice in each scientific community.

PREFACE

This book contains all manuscripts approved by the reviewers and the organizing committee of the 12th International Conference on Computational Fluid Dynamics in the Oil & Gas, Metallurgical and Process Industries. The conference was hosted by SINTEF in Trondheim in May/June 2017 and is also known as CFD2017 for short. The conference series was initiated by CSIRO and Phil Schwarz in 1997. So far the conference has been alternating between CSIRO in Melbourne and SINTEF in Trondheim. The conferences focuses on the application of CFD in the oil and gas industries, metal production, mineral processing, power generation, chemicals and other process industries. In addition pragmatic modelling concepts and bio-mechanical applications have become an important part of the conference. The papers in this book demonstrate the current progress in applied CFD.

The conference papers undergo a review process involving two experts. Only papers accepted by the reviewers are included in the proceedings. 108 contributions were presented at the conference together with six keynote presentations. A majority of these contributions are presented by their manuscript in this collection (a few were granted to present without an accompanying manuscript).

The organizing committee would like to thank everyone who has helped with review of manuscripts, all those who helped to promote the conference and all authors who have submitted scientific contributions. We are also grateful for the support from the conference sponsors: ANSYS, SFI Metal Production and NanoSim.

Stein Tore Johansen & Jan Erik Olsen

Organizing committee:

Conference chairman: Prof. Stein Tore Johansen
Conference coordinator: Dr. Jan Erik Olsen
Dr. Bernhard Müller
Dr.Sigrid Karstad Dahl
Dr.Shahriar Amini
Dr.Ernst Meese
Dr.Josip Zoric
Dr.Jannike Solsvik
Dr.Peter Witt

Scientific committee:

Stein Tore Johansen, SINTEF/NTNU
Bernhard Müller, NTNU
Phil Schwarz, CSIRO
Akio Tomiyama, Kobe University
Hans Kuipers, Eindhoven University of Technology
Jinghai Li, Chinese Academy of Science
Markus Braun, Ansys
Simon Lo, CD-adapco
Patrick Segers, Universiteit Gent
Jiyuan Tu, RMIT
Jos Derksen, University of Aberdeen
Dmitry Eskin, Schlumberger-Doll Research
Pär Jönsson, KTH
Stefan Pirker, Johannes Kepler University
Josip Zoric, SINTEF

CONTENTS

VERIFICATION OF FILTERED TWO FLUID MODELS FOR REACTIVE GAS-SOLID FLOWS

Jan Hendrik CLOETE[1], Schalk CLOETE[2], Stefan RADL[3], Shahriar AMINI[1,2*]

[1] Department of Energy and Process Engineering, Norwegian University of Science and Technology (NTNU), 7491 Trondheim, NORWAY

[2] Flow Technology Department, SINTEF Materials and Chemistry, NO-7465 Trondheim, NORWAY

[3] Institute of Process and Particle Engineering, Graz University of Technology, Graz, AUSTRIA

*Corresponding author's e-mail: shahriar.amini@sintef.no

ABSTRACT

CFD simulations of fluidized bed reactors are generally limited to the laboratory scale because of the fine grid sizes that are required to resolve complex particle clustering phenomena. The filtered Two Fluid Model (fTFM) approach has recently emerged as a promising method for allowing reasonable predictions of large-scale fluidized beds. This paper presents a verification study of new two-marker fTFM closures. In general, the fTFMs matched well to the resolved simulations. It was shown that the two-marker models significantly increased the predicted degree of phase segregation (resolved in coarse grid simulations), and hence have superior capabilities compared to simpler one-marker models. Also, the two-marker model predicted a more dynamic transient flow behaviour. However, further work is recommended to extend the present study over a wider range of flow conditions.

Keywords: CFD, Fluidized beds, verification, filtered two-fluid model.

NOMENCLATURE

Greek Symbols

α Volume fraction, [].
μ Dynamic viscosity, [kg/m·s].
ρ Density, [kg/m^3].
$\overline{\overline{\tau}}_s$ Stress tensor, [Pa].
υ Velocity, [m/s].
Δ_f Filter size, [m].

Latin Symbols

d Particle diameter, [m].
D Mass diffusivity, [m^2/s].
g Gravitational acceleration, [m/s^2].
K_{sg} Momentum exchange coefficient, [kg/m^{3}s].
p Pressure, [Pa].
S Shear rate magnitude, [1/s].
t Time, [s].
v_t Terminal settling velocity, [m/s].
X_A Mass fraction of species A, [].

Subscripts, superscripts and accents

f Filtered.
g Gas.
s Solids.
$\overline{\ }$ Algebraic volume average.
$\widetilde{\ }$ Phase-weighted volume average.
$\langle\ \rangle$ Time average.
$\vec{\ }$ Vector quantity.
* Scaled or non-dimensionalized quantity.
$'$ Fluctuating quantity.

INTRODUCTION

Fluidized beds are widely used in industry due to their excellent mass and heat transfer properties. In the last three of decades, CFD has emerged as a useful tool with which to investigate the reactive flow in these reactors, although significant challenges remain (Cloete et al., 2012). The most important limitation of this approach remains the excessive computational times involved in simulating industrial scale reactors, due to the large number of particles (in the order of 10^{12}).

The filtered Two-Fluid Model (fTFM) (Igci et al., 2008) offers a solution to this problem. The TFM closed by the Kinetic Theory of Granular Flow (KTGF) (Lun et al., 1984, Gidaspow et al., 1992), where the fluctuations in the particle velocities are treated analogous to that of gas molecules in the kinetic theory of gases, are often employed in fluidized bed simulations. However,

KTGF-based TFMs suffer from the limitation that they require a high enough grid resolution to resolve the small scale structures (particle clusters and gas bubbles) for accurate model predictions, leading to computationally expensive simulations. The fTFM aims to reduce the required computational time substantially by relying on spatially-averaged (i.e., "filtered") governing equations. However, this leads to additional terms in these equations (that account for small-scale fluctuations) which must be closed. These closures are generally formulated as a function of the size of the averaging region, and additional marker quantities. Closures may be obtained by fitting a proposed functional form to data obtained from fine grid TFM simulations.

Most of the research in this field has been limited to developing models for the filtered hydrodynamics (Ozel et al., 2013, Schneiderbauer and Pirker, 2014, Sarkar et al., 2016), where sub-grid corrections to the interphase drag and solids stresses are essential. However, in reactive flows further closures are required to correct the reaction rate and species dispersion for sub-grid effects. Models have been proposed for these effects (Holloway and Sundaresan, 2012, Agrawal et al., 2013), but have not been verified so far.

This paper will therefore evaluated the reactive fTFM closures developed by the Princeton group (Igci and Sundaresan, 2011, Holloway and Sundaresan, 2012, Agrawal et al., 2013). Additionally, a new set of closures for the filtered drag, solids pressure and reaction rate will be tested. These comparisons will give an indication of the ability of the fTFM approach to predict reactive flow on coarse grids and will help identify areas of improvement for the existing models.

MODEL DESCRIPTION

Governing equations

Two types of simulations are performed in this study: coarse grid simulations using fTFM closures and resolved TFM simulations against which to verify the coarse grid results. The resolved TFM simulations follow a standard KTGF approach as commonly employed in the literature, e.g. (Cloete et al., 2017), and the equations and closures used will therefore not be described here in detail.

However, the equations and fTFM closures employed in the coarse grid simulations warrant further discussion. Two sets of fTFM closures are evaluated in this verification study: a model from the Princeton group and a new model proposed in this study. To derive filtered equations, a spatial average is performed on all equations and averages of products are rearranged by defining the instantaneous value of a quantity as the sum of its averaged value and a fluctuating component. Employing this procedure to the solids momentum equation, the following equation is obtained.

$$\begin{aligned}&\frac{\partial}{\partial t}\left(\rho_s\overline{\alpha_s}\widetilde{\upsilon_s}\right)+\nabla\cdot\left(\rho_s\overline{\alpha_s}\widetilde{\upsilon_s}\widetilde{\upsilon_s}\right)=-\overline{\alpha_s}\nabla\overline{p}-\nabla\overline{p_s}\\&-\nabla\cdot\left(\rho_s\overline{\alpha_s\upsilon_s'\upsilon_s'}\right)+\nabla\cdot\overline{\overline{\tau}_s}+\overline{\alpha_s}\rho_s\vec{g}+\overline{K_{gs}\left(\upsilon_g-\upsilon_s\right)}-\overline{\alpha_s'\nabla p'}\end{aligned}\qquad(1)$$

For the hydrodynamics, closures are required for the filtered kinetic theory stresses (second term and fourth term on the right), the meso-scale solids stresses (third term on the right), the filtered drag force (sixth term on the right) and an added mass-like force due to the subgrid pressure gradient fluctuations (last term on the right). Additionally, similar meso-scale stresses in the gas momentum equation will require closure. However, in this study these stresses are neglected, since they are generally considered to be much smaller than the particle phase meso-scale stresses (Milioli et al., 2013).

For the fTFM hydrodynamics from the Princeton group, the model by Igci and Sundaresan (2011) is used, which closes the filtered solids stresses and the filtered drag as a function of the filter size and the filtered solids volume fraction. Although more advanced models using an additional marker have been published, a recent hydrodynamic verification study (Cloete et al., 2017) showed that these advanced models perform poorly in predicting the hydrodynamics in 2D flows, whereas the simpler Igci model performed very well.

For the fTFM proposed in this study, the following closures are suggested. The filtered drag force and the pressure gradient fluctuation term are modelled together as a correction to the microscopic drag law, as follows.

$$C=\frac{\overline{K_{gs}\left(\upsilon_{g,i}-\upsilon_{s,i}\right)-\alpha_s'\dfrac{dp'}{dx_i}}}{K_{gs,microscopic}\left(\widetilde{\upsilon}_{g,i}-\widetilde{\upsilon}_{s,i}\right)}\qquad(2)$$

The drag correction factor, C, is calculated as a function of the dimensionless filter size (Igci et al., 2008), the filtered solids volume fraction and the filtered slip velocity magnitude scaled by the steady state slip velocity (Cloete et al.). This scaling of the slip velocity was shown to lead to a better distribution of data in the parameter space and to a simple dependency of the drag correction factor on the filtered slip velocity, resulting in a better fit of the correlation to the resolved simulation data. The following correlation is used:

$$-\log(C)=\begin{pmatrix}\operatorname{atan}\left(x_1\left(\Delta_f^*-\Delta_{fine}^*\right)^{x_9}\overline{\alpha}_s\right)\times\\\operatorname{atan}\left(\begin{matrix}x_2\left(\Delta_f^*-\Delta_{fine}^*\right)^{x_{10}}\times\\\left(\overline{\alpha}_{\max}-\overline{\alpha}_s\right)\end{matrix}\right)\times\\\operatorname{atan}\left(x_3\left(\Delta_f^*-\Delta_{fine}^*\right)\right)\times\\\left(\begin{matrix}x_4\log\widetilde{\upsilon}_{slip}^*+x_5\left(\Delta_f^*-\Delta_{fine}^*\right)^{x_6}+\\x_7(\log\widetilde{\upsilon}_{slip}^*)^2(1-\\\operatorname{atan}\left(x_8\left(\Delta_f^*-\Delta_{fine}^*\right)\right)\Big/\left(\frac{\pi}{2}\right)\end{matrix}\right)\end{pmatrix}\Bigg/\left(\frac{\pi}{2}\right)^3\qquad(3)$$

Where $x_1=46.75$, $x_2=51.51$, $x_3=1.370$, $x_4=0.8632$, $x_5=0.05360$, $x_6=0.4776$, $x_7=364.1$, $x_8=260.7$, $x_9=0.889$, $x_{10}=0.494$, and $\bar{\alpha}_{max}=0.55$. The fine grid scaled filter size is set to $\Delta_{fine}^*=0.1286$.

It is assumed that the filtered kinetic theory stresses are much smaller than the meso-scale stresses for filter sizes large enough for practical use (Igci et al., 2008). Therefore closures for the former stresses are neglected. However, the following closure is proposed for the

dimensionless filtered frictional pressure, which was found to be significant:

$$\frac{p_{s,fric}}{\rho_s v_t^2} = \bar{\alpha}_s^{x_1}\left(\Delta_f^* - \Delta_{fine}^*\right)^{x_2} \times \left(x_3 \bar{S}_s^{*x_4}\left(\Delta_f^* - \Delta_{fine}^*\right)^{x_5} + x_6 \frac{\bar{\alpha}_s^{x_7}}{(\alpha_{s,\max} - \bar{\alpha}_s)^{x_8}}\right) \quad (4)$$

Where $x_1 = 4.016$, $x_2 = -0.005543$, $x_3 = 0.1905$, $x_4 = 1.939$, $x_5 = 1.658$, $x_6 = 0.03935$, $x_7 = 12.78$, $x_8 = 5.084$ and $\bar{\alpha}_{s,max} = 0.63$. The dimensionless filtered solids shear rate magnitude, $\bar{S}_s^*$, is calculated as done by Milioli et al. (2013).

It was found that the effect of modelling the off-diagonal component of the solids meso-scale stress on the coarse grid simulations were small, therefore a new model was not derived as part of this study and the model of (Sarkar et al., 2016) is used. For the diagonal components of the solids meso-scale stresses the following correlation is proposed:

$$\frac{\rho_s \overline{\alpha_s \upsilon'_{s,x} \upsilon'_{s,x}}}{\rho_s v_t^2} = \frac{\rho_s \overline{\alpha_s \upsilon'_{s,y} \upsilon'_{s,y}}}{\rho_s v_t^2} = \bar{\alpha}_s^{x_1} \operatorname{atan}(x_2(\alpha_{\max} - \bar{\alpha}_s)) \times \left(\Delta_f^* - \Delta_{fine}^*\right)^{x_3}\left(x_4 \bar{S}_s^{*x_5} + x_6 \bar{\alpha}_s^{x_7}\right) \Big/ \left(\frac{\pi}{2}\right) \quad (5)$$

Where $x_1 = 1.522$, $x_2 = 15.49$, $x_3 = 1.162$, $x_4 = 0.5660$, $x_5 = 1.385$, $x_6 = 0.07166$, $x_7 = -0.9543$, and $\bar{\alpha}_{max} = 0.6043$. The correlation shape is based on a Smagorinsky-type model as used by Sarkar et al. (2016), with modifications to have zero meso-scale stresses at the filter size where the resolved simulations were performed, and non-zero meso-scale stresses at zero filtered shear rates. The latter is motivated by an observation of Schneiderbauer (2016).

A simple irreversible, first-order, solids-catalysed reaction of species A to species B is considered in this study. The filtered gas species transport equation, formulated for the mass fraction of species A, is:

$$\frac{\partial}{\partial t}\left(\rho_g \overline{\alpha_g \widetilde{X_A}}\right) + \nabla \cdot \left(\rho_g \overline{\alpha_g} \widetilde{X_A} \widetilde{\upsilon_g}\right) = \nabla \cdot (D \overline{\alpha_g \rho_g \nabla X_A}) - \nabla \cdot \left(\rho_g \overline{\alpha_g X_A' \upsilon_g'}\right) - k_A \rho_g \overline{\alpha_s X_A} \quad (6)$$

The first term on the right is neglected, considering that the molecular diffusion is small relative to species dispersion due to the meso-scale velocity fluctuations (i.e., the second term on the right). The species dispersion due to the meso-scale velocity fluctuations is modelled as an added diffusivity as proposed by Agrawal et al. (2013).

The last term on the right hand side of the species transport equation is modelled as follows:

$$\overline{\alpha_s X_A} = R \overline{\alpha_s} \widetilde{X_A} \quad (7)$$

The reaction rate correction factor R accounts for the effect of unresolved concentration and voidage fluctuations on the filtered reaction source term. It can be calculated from finely-resolved reaction rate data, and can be defined such that it also accounts for non-local effects (i.e., gradient terms) as suggested by Holloway and Sundaresan (2012). This was also done in our present contribution. For the Princeton fTFM setup the model by Holloway and Sundaresan (2012) is used. A new model for R, adding an additional marker for the scaled slip velocity, is proposed as part of this study. The proposed model is limited to the specific case of a reaction rate constant giving a Thiele modulus of 0.16.

$$-\log(R) = \operatorname{atan}\left(x_1\left(\Delta_f^* - \Delta_{fine}^*\right)^{x_7} \bar{\alpha}_s\right) \times \operatorname{atan}\left(x_2\left(\Delta_f^* - \Delta_{fine}^*\right)^{x_8} \times (\bar{\alpha}_{\max} - \bar{\alpha}_s)\right) \times \left(\frac{\operatorname{atan}(x_4 \tilde{\upsilon}_{slip}^*)}{\operatorname{atan}\left(x_3\left(\Delta_f^* - \Delta_{fine}^*\right)\right)} \times x_5 \log \tilde{\upsilon}_{slip}^* + x_6\right) \Big/ \left(\frac{\pi}{2}\right)^3 \quad (8)$$

Where $x_1 = 7.925$, $x_2 = 17.31$, $x_3 = 0.3511$, $x_4 = 0.7772$, $x_5 = 0.1366$, $x_6 = 1.007$, $x_7 = -0.09253$, $x_8 = -0.003722$ and $\bar{\alpha}_{max} = 0.5627$.

Verification cases

The average superficial inlet gas velocity for this study is chosen to be at the geometric center of the bubbling fluidization regime, according to Bi and Grace (1995), giving an average superficial velocity of $0.468\,\frac{m}{s}$ at the inlet. A solids flux of $150\,\frac{kg}{m^2 s}$ is specified.

Furthermore, the profile of the velocity, solids volume fraction and reactant mass fraction at the inlet is specified to be non-uniform. This allows more rigorous testing of the filtered models by creating mean gradients in the flow. The gas phase superficial velocity is chosen to be half the average superficial velocity at the sides of the domain and increases linearly towards the center. Zero slip between the phases is specified at the inlet. The solid volume fraction is set to a minimum at the centre and increases linearly to the sides. The value of the minimum solids volume fraction is set equal to half the solids volume fraction required to deliver the specified solids flux at the mean gas superficial velocity. Finally, the reactant species mass fraction is set to 1 at the center and 0 at the sides.

The simulation domain consists of a rectangular reactor region, 0.96 m by 1.6 m, and a small outlet region with walls sloping at 45° towards the outlet. The wall boundary condition is set as free slip for the solids to minimize the effect of the outlet region on the flow in the rest of the domain. The outlet has a small width of 10 cm to prevent backflow, which could potentially cause numerical instabilities. The sides of the fluidization region are specified as periodic boundaries, since the models evaluated in this study was derived for periodic flows far away from wall-effects.

Due to the large computational expense of performing resolved simulations (performed at a grid size equal to

11.8 times the particle diameter) in such a large domain, all simulations were performed in 2D. Testing filtered models in 2D remains a valid approach, since filtered models derived from 2D and 3D simulations have been shown to be qualitatively similar (Igci et al., 2008).

The particle and fluid properties used in the simulations are summarized in Table 1.

Table 1: Summary of particle and fluid properties

d	Particle diameter	75×10^{-6} m
ρ_s	Particle density	1500 kg/m^3
ρ_g	Gas density	1.3 kg/m^3
μ_g	Gas viscosity	1.8×10^{-5} kg/m s
v_t	Terminal settling velocity	0.2184 m/s
D	Mass diffusivity	1.385×10^{-5} m^2/s

The coarse grid simulations are allowed to run for 10 s of simulation time to reach a statistical steady state, after which the results are time averaged for 50 s. The resolved simulation has been time-averaged for 9 s. Two values are used to quantify the overall reactor behaviour: the average solids holdup and the average scaled conversion. The average solids holdup is calculated as the time-averaged solids volume fraction averaged over the rectangular region of the geometry. The scaled conversion of the reactant is calculated as $-\log_{10}\langle X_A\rangle$. To calculate $\langle X_A\rangle$ the time-average reactant mass fraction is averaged over a horizontal line at a height of 1.5 m (0.1 m below the start of the outlet region). The averaging regions for both quantities are chosen in such a way as to minimize the effect of the outlet region on the results.

RESULTS

Results will be presented and discussed in two main sections. Firstly, the overall model performance will be compared using the holdup and conversion performance parameters discussed in the previous paragraph. Then, a more detailed comparison between the different model predictions for the spatial distribution of key quantities will be presented and discussed.

Overall comparison

Model performance is summarized in Figure 1. Firstly, the need for filtered modelling on coarse grids is readily visible from the cases without any filtered models. Predictions of the holdup without any filtered modelling are lower by about 20% because clusters are not resolved and drag is over-predicted. A much larger error is observed for the reaction rate because mass transfer limitations caused by clustering are strongly under-predicted when not resolving the clusters. It is notable that the overall conversion is over-predicted by up to 100% even though a substantially lower solids holdup is predicted.

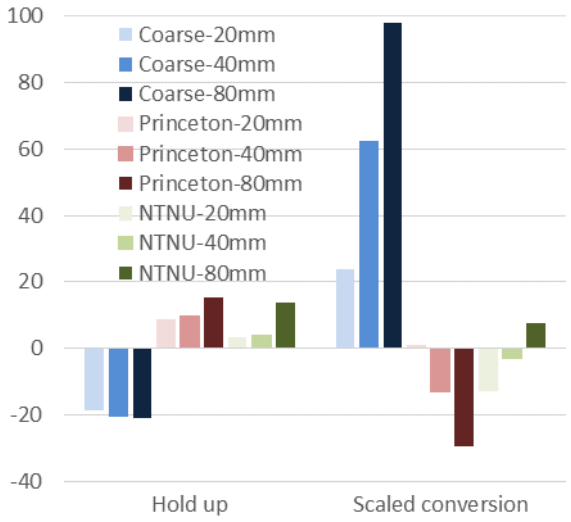

Figure 1: Deviation of model predictions from the resolved simulations for the solids holdup and reactant conversion.

Both filtered models investigated in this work resulted in substantial improvements relative to the cases without any filtered modelling. However, it is also clear that both models show significant grid dependencies, implying that work is still needed to improve the filter size dependency on the models. The primary difference between the performance of the Princeton and NTNU model setups is the trend of reactant conversion with an increase in grid size. The Princeton model increasingly under-predicts the reactant conversion at larger grid sizes, whereas the NTNU model over-predicts it. For the NTNU model, this trend is aligned with the increase in solids holdup at larger filter sizes, so the trend can be partly explained by the imperfect hydrodynamic models. For the Princeton models, on the other hand, the trend is in opposition to the holdup trend, implying that significant improvements to the reaction rate model are required.

Detailed comparison

A good idea about model behaviour can be formed by inspecting the contours of instantaneous solids volume fraction and conversion presented in Figure 2 and Figure 3.

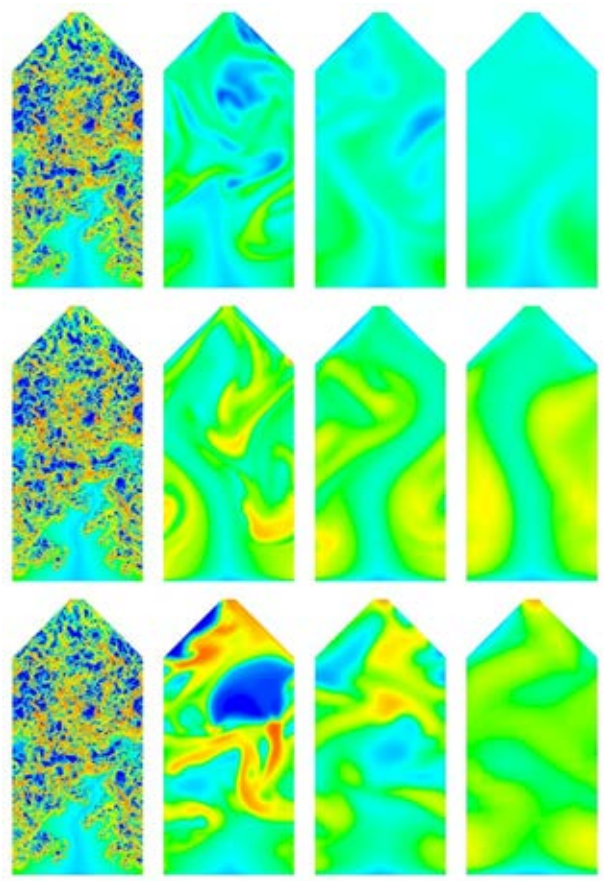

Figure 2: Instantaneous contours of solids volume fraction. Top row: no filtered modelling. Middle row: Princeton model. Bottom row: NTNU model. Each row shows the resolved simulation on the left and then the coarse grid simulations on grids of 20, 40 and 80 mm. The blue-red colour map spans a range of 0-0.6.

Figure 2 clearly shows the increased holdup simulated by the filtered models relative to the coarse grid simulations with no filtered modelling. In addition, the NTNU models (two-marker models) generally predict more phase segregation than the Princeton models (i.e., primarily one-marker models). This is the result of a wider range of variation for each filtered quantity ensured by a two-marker model relative to a one-marker model. The variation of filtered quantities (e.g. drag, pressure, etc.) will therefore be more pronounced in adjacent cells and the resulting force gradients will lead to greater phase segregation. As expected, it is also clearly visible that the amount of phase segregation reduces as the grid size (and filter size) is increased.

When inspecting the resolved simulation profiles, it appears as if the prediction of denser "clusters of clusters" by the filtered model is correct. Denser regions with many clusters and more dilute regions with fewer clusters are clearly visible in the resolved simulation. The resolution of these denser regions is gradually lost as the grid size is increased in the filtered simulations, especially for the one-marker Princeton models.

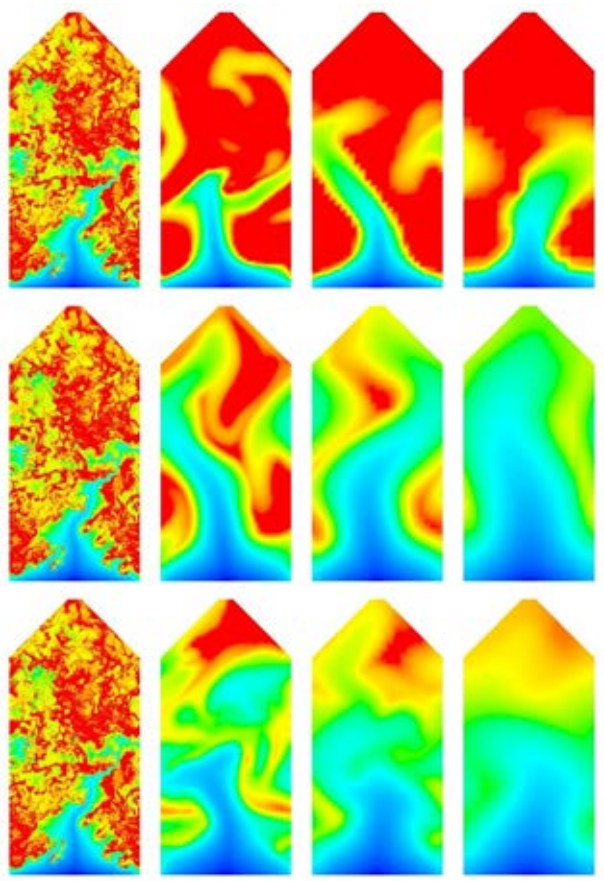

Figure 3: Instantaneous contours of reactant conversion $\left(-\mathbf{log_{10}}\overline{\langle X_A \rangle}\right)$. Top row: no filtered modelling. Middle row: Princeton model. Bottom row: NTNU model. Each row shows the resolved simulation on the left and then the coarse grid simulations on grids of 20, 40 and 80 mm. The blue-red colour map spans a range of 0-7.

The reactant conversion profiles in Figure 3 show that the filtered models generally capture the reactant transport correctly: low conversion in the central part of the inlet (high velocities and reactant mole fractions, and low volume fractions) with higher conversions at the sides of the domain. In addition, regions of low and high conversion in the developed flow regions seem to be qualitatively captured by the filtered models. As may be expected, these regions are aligned with the regions of low and high solids volume fraction in Figure 2.

It should be noted that the conversion looks misleadingly low in the filtered simulations because of the log scaling used to visualize the conversion. Spatial averages over a range of conversions $\left(-\log_{10}\overline{\langle X_A \rangle}\right)$ would be heavily weighted towards lower sample values.

Another perspective is given by the time-averaged solids volume fraction and conversion plots given in Figure 4 and Figure 5. The solids volume fraction contours show that the Princeton models generally predict higher solids volume fraction regions on the sides of the domain than the NTNU models. This is accentuated as the grid size is increased until a central spout between two dense regions is predicted on the 80 mm grid. In this measure, the NTNU models appear to match more closely with the resolved simulations,

although the triangular shape of the central inlet spout is gradually lost as the grid size is increased.

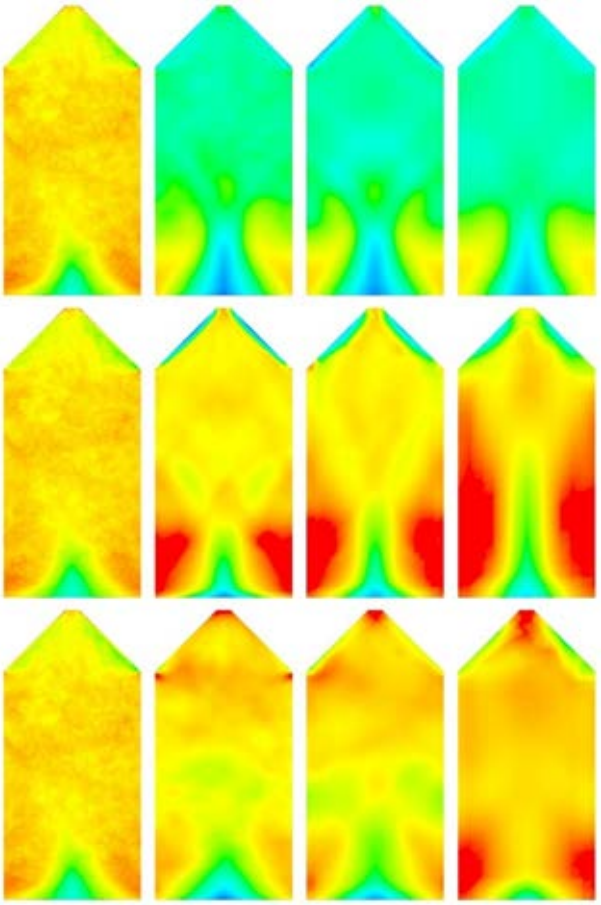

Figure 4: Time-averaged contours of solids volume fraction. Top row: no filtered modelling. Middle row: Princeton model. Bottom row: NTNU model. Each row shows the resolved simulation on the left and then the coarse grid simulations on grids of 20, 40 and 80 mm. The blue-red colour map spans a range of 0.1-0.36.

In general, it appears as if dense regions over the sides of the inlet tend to form more easily when less flow dynamics (driven primarily by phase segregation) are resolved. This may be expected since dynamically moving dense regions will have a lower tendency to stagnate in regions with low fluidization velocity, but rather move through that region to again be swept up by the stronger central gas stream. The greater phase segregation resolved by the two-marker NTNU models therefore appears to improve the prediction in this case.

When inspecting the reactant conversion contours in Figure 5, it is seen that the profiles qualitatively align with the volume fraction profiles in Figure 4: denser regions align with higher conversion and vice versa. However, significant improvement still seems to be possible. Both models appear to under-predict the conversion in the bottom-side regions of the domain. The Princeton models over-predicted solids holdup in these regions, so it would be expected that a similar over-prediction in conversion will result. This becomes particularly evident at larger filter sizes where large regions of high volume fraction were predicted, but conversion is increasingly under-predicted. Similarly, the NTNU models predict the solids holdup with reasonable accuracy in the bottom-side regions of the domain, but the conversion in these regions is significantly under-predicted. This may be related to a over-prediction of the scalar dispersion rate.

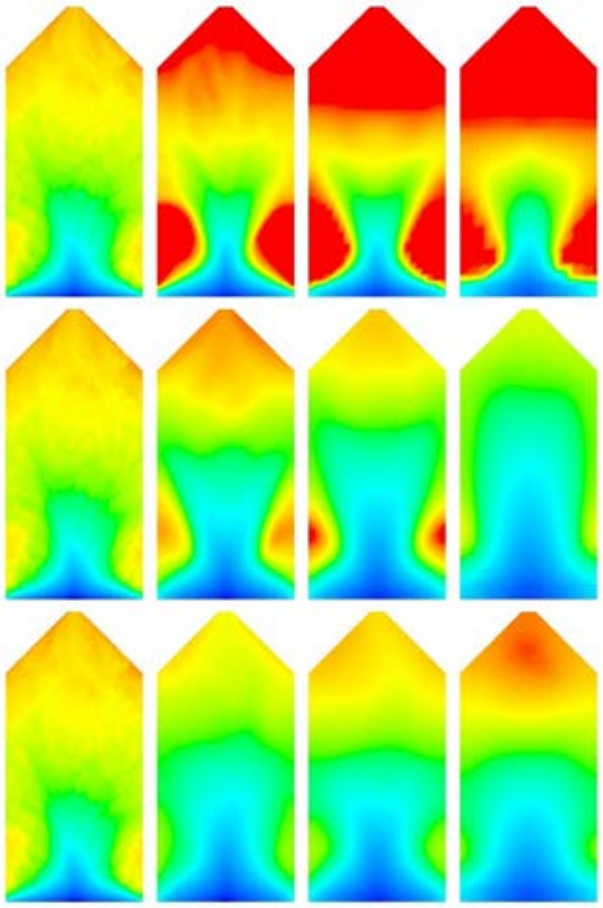

Figure 5: Time-averaged contours of reactant conversion $\left(-\mathbf{log_{10}}\overline{\langle X_A \rangle}\right)$. Top row: no filtered modelling. Middle row: Princeton model. Bottom row: NTNU model. Each row shows the resolved simulation on the left and then the coarse grid simulations on grids of 20, 40 and 80 mm. The blue-red colour map spans a range of 0-6.

As shown in Figure 6, exclusion of the scalar dispersion model led to a reactant conversion profile that is better aligned with the solids volume fraction profiles shown in Figure 4. The dense regions at the sides of the domain above the inlet now show greater conversion. However, the effect of the scalar dispersion model is small and it did not significantly affect the overall conversion in the domain.

Aside from this moderate discrepancy in the lateral direction at the bottom of the domain, conversion also appears to proceed too slowly along the height of the domain despite reasonably accurate predictions of the solids volume fraction in Figure 4. For the NTNU model, one possible explanation for this trend is that the phase segregation is too strong, leading to excessive mass transfer limitations. Further investigation is required to determine whether these moderate discrepancies are caused by inaccuracies from the hydrodynamic models or the reaction rate model. Given the relative simplicity of deriving a reaction rate model, the hydrodynamic models appear to be the more likely source of error. For the Princeton models, the filter size

dependency of the reaction rate model appears to be too weak, leading to progressively larger under-predictions of conversion with an increase in the grid size.

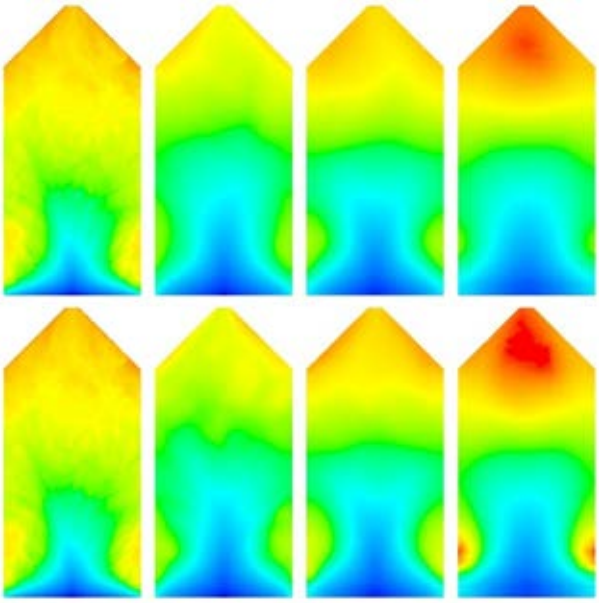

Figure 6: Time-averaged contours of reactant conversion $(-\boldsymbol{log}(\boldsymbol{X_A}))$ with the NTNU model. Top row: with scalar dispersion model. Bottom row: without scalar dispersion model. Each row shows the resolved simulation on the left and then the coarse grid simulations on grids of 20, 40 and 80 mm. The blue-red colour map spans a range of 0-6.

CONCLUSION

A new two-marker filtered Two Fluid Model formulation is presented for solving reactive flows in fluidized beds. The model is verified against a computationally expensive resolved simulation to show good agreement. However, significant grid dependency is still present, which must be addressed in future model development work.

The two-marker model is compared to earlier one-marker models from the literature. Greater phase segregation is resolved by the two-marker model relative to the one-marker model, thereby capturing more flow dynamics even on a coarse mesh. In this case, the increased resolution of flow prevented excessive stagnation in low velocity regions of the domain.

The proposed two-marker reaction rate model performed significantly better than the existing one-marker model where the filter size dependency was found to be too weak. It is likely that the required improvements to conversion predictions can be more readily achieved by improving the more complex hydrodynamic models than the relatively simple reaction rate model. Finally, it was found that the inclusion of a model for dispersion of the reactant due to meso-scale velocity fluctuations appeared to have a slightly negative effect on model accuracy.

In general, this successful verification study shows the promise of the two-marker model approach. Further verification work over a wider range of flow conditions is recommended for future study.

ACKNOWLEDGEMENTS

The authors would like to express their gratitude for the financial support from the European Commission under the NanoSim grant (project number: 604656), as well as for the computational resources provided at NTNU by UNINETT Sigma2 AS, https://www.sigma2.no.

REFERENCES

AGRAWAL, K., HOLLOWAY, W., MILIOLI, C. C., MILIOLI, F. E. and SUNDARESAN, S., (2013), "Filtered models for scalar transport in gas–particle flows", *Chem. Eng. Sci.*, **95** (0), 291-300.

BI, H. T. and GRACE, J. R., (1995), "Flow regime diagrams for gas-solid fluidization and upward transport", *Int. J. Multiphase Flow*, **21** (6), 1229-1236.

CLOETE, J. H., CLOETE, S., MUNICCHI, F., RADL, S. and AMINI, S., (2017), "The sensitivity of filtered Two Fluid Model to the underlying resolved simulation setup", *Powder Technol.*

CLOETE, J. H., CLOETE, S., RADL, S. and AMINI, S. (2017). "Verification of filtered Two-Fluid Models in different flow regimes", *CFB-12*.Krakow.

CLOETE, J. H., CLOETE, S., RADL, S., MUNICCHI, F. and AMINI, S., "A new anisotropic drag closure for filtered Two Fluid Models", *AIChE J.*, **Submitted**.

CLOETE, S., JOHANSEN, S. T. and AMINI, S., (2012), "An assessment of the ability of computational fluid dynamic models to predict reactive gas–solid flows in a fluidized bed", *Powder Technol.*, **215-216** (0), 15-25.

GIDASPOW, D., BEZBURUAH, R. and DING, J., (1992), "Hydrodynamics of Circulating Fluidized Beds, Kinetic Theory Approach", *7th Engineering Foundation Conference on Fluidization* 75-82.

HOLLOWAY, W. and SUNDARESAN, S., (2012), "Filtered models for reacting gas–particle flows", *Chem. Eng. Sci.*, **82** (0), 132-143.

IGCI, Y., ANDREWS, A. T., SUNDARESAN, S., PANNALA, S. and O'BRIEN, T., (2008), "Filtered two-fluid models for fluidized gas-particle suspensions", *AIChE J.*, **54** (6), 1431-1448.

IGCI, Y. and SUNDARESAN, S., (2011), "Constitutive Models for Filtered Two-Fluid Models of Fluidized Gas–Particle Flows", *Ind. Eng. Chem. Res.*, **50** (23), 13190-13201.

LUN, C. K. K., SAVAGE, S. B., JEFFREY, D. J. and CHEPURNIY, N., (1984), "Kinetic Theories for Granular Flow: Inelastic Particles in Couette Flow and Slightly Inelastic Particles in a General Flow Field", *J. Fluid Mech.*, **140**, 223-256.

MILIOLI, C. C., MILIOLI, F. E., HOLLOWAY, W., AGRAWAL, K. and SUNDARESAN, S., (2013), "Filtered two-fluid models of fluidized gas-particle flows: New constitutive relations", *AIChE J.*, **59** (9), 3265-3275.

OZEL, A., FEDE, P. and SIMONIN, O., (2013), "Development of filtered Euler–Euler two-phase model for circulating fluidised bed: High resolution simulation, formulation and a priori analyses", *Int. J. Multiphase Flow*, **55** (0), 43-63.

SARKAR, A., MILIOLI, F. E., OZARKAR, S., LI, T., SUN, X. and SUNDARESAN, S., (2016), "Filtered sub-grid constitutive models for fluidized gas-particle flows constructed from 3-D simulations", *Chem. Eng. Sci.*, **152**, 443-456.

SCHNEIDERBAUER, S., (2016), "Cluster induced turbulence (CIT) - A spatially averaged two-fluid model (SA-TFM) for dense gas-solid flows", *24th ERCOFTAC ADA Pilot Center Meeting*.

SCHNEIDERBAUER, S. and PIRKER, S., (2014), "Filtered and heterogeneity-based subgrid modifications for gas–solid

drag and solid stresses in bubbling fluidized beds", *AIChE J.*, **60** (3), 839-854.